

# Lawrence Berkeley National Laboratory

## Lawrence Berkeley National Laboratory

### Title

Jets and dijets in Au+Au and p+p collisions at RHIC

### Permalink

<https://escholarship.org/uc/item/34p2t50p>

### Authors

Hardtke, D.  
STAR Collaboration

### Publication Date

2002-12-09

# Jets and Dijets in Au+Au and p+p Collisions at RHIC

David Hardtke<sup>a</sup> for the STAR Collaboration\*

<sup>a</sup>Nuclear Science Division  
Lawrence Berkeley National Laboratory  
Berkeley, CA 94720

Recent data from RHIC suggest novel nuclear effects in the production of high  $p_T$  hadrons. We present results from the STAR detector on high  $p_T$  angular correlations in Au+Au and p+p collisions at  $\sqrt{s} = 200$  GeV/c. These two-particle angular correlation measurements verify the presence of a partonic hard scattering and fragmentation component at high  $p_T$  in both central and peripheral Au+Au collisions. When triggering on a leading hadron with  $p_T > 4$  GeV, we observe a quantitative agreement between the jet cone properties in p+p and all centralities of Au+Au collisions. This quantitative agreement indicates that nearly all hadrons with  $p_T > 4$  GeV/c come from jet fragmentation and that jet fragmentation properties are not substantially modified in Au+Au collisions. STAR has also measured the strength of back-to-back high  $p_T$  charged hadron correlations, and observes a small suppression of the back-to-back correlation strength in peripheral collisions, and a nearly complete disappearance of back-to-back correlations in central Au+Au events. These phenomena, together with the observed strong suppression of inclusive yields and large value of elliptic flow at high  $p_T$ , are consistent with a model where high  $p_T$  hadrons come from partons created near the surface of the collision region, and where partons that originate or propagate towards the center of the collision region are substantially slowed or completely absorbed.

## 1. Introduction

At high energy density, nuclear matter may undergo a phase transition to a deconfined state consisting of free quarks and gluons. This Quark-Gluon Plasma may be experimentally accessible using the collisions of heavy nuclei at high energies. In order to investigate this new state of matter, processes whose rates are calculable in the absence of nuclear effects are particularly useful. The production of large transverse momentum jets, in the limit of no nuclear effects, should scale with the number of binary nucleon-nucleon collisions with a rate calculable from perturbative QCD. A deviation from this binary scaling expectation for jet production or a modification of jet properties would indicate the presence of initial and/or final state nuclear effects. The final state nuclear effects are of particular interest since they may be used to verify the presence of a Quark-Gluon plasma and may probe the properties of the plasma.

---

\*For the full author list and acknowledgements, see Appendix “Collaborations” of this volume.

A large momentum parton traversing a dense gluonic system may lose energy due to collisions or induced gluon radiation [1,2]. The rate of energy loss ( $dE/dx$ ) is expected to scale with the density of the gluonic system. Both PHENIX and STAR have measured the single inclusive hadron yields at high  $p_T$  and found a suppression compared to the binary nucleon-nucleon scaling expectation [3,4]. While these measurements are consistent with energy loss in a dense gluonic system, the particle production mechanism for high  $p_T$  hadrons in central Au+Au collisions may be different than in elementary collisions. Indeed, the ratio of proton to pion at large  $p_T$  ( $\approx 2 - 4$  GeV/c) has been measured by the Phenix collaboration to be near unity in central Au+Au collisions, compared to a ratio of  $\approx 0.2$  measured in p+p collisions [5]. This has been interpreted by some as an indication of a large hydrodynamical type contribution to the charged hadron yield in Au+Au collisions, even at rather large  $p_T$ . The present work addresses the particle production mechanism at high  $p_T$  using two-particle azimuthal correlations. We show that hard scattering and fragmentation is the dominant particle production mechanism for  $p_T > 4$  GeV/c. In addition, we show that back-to-back dihadrons, a signature of dijets, are suppressed in the most central Au+Au collisions.

## 2. Experiment and Method

Partons fragment into jets of hadrons around the direction of parton propagation. Due to the large multiplicities in central Au+Au collisions at RHIC, full jet reconstruction is difficult. To identify jets on a statistical basis, STAR utilizes two-hadron azimuthal correlations at large transverse momentum. The STAR experiment has been described in detail elsewhere [6], so only details particularly relevant to this analysis are given. The main tracking detector is a large acceptance Time Projection Chamber with full azimuthal coverage and large pseudo-rapidity acceptance ( $|\eta| < 1.5$ ). The TPC resides in a 0.5T solenoidal magnet. The trajectories of charged tracks are measured in the TPC, and the interaction vertex is reconstructed on an event-by-event basis. The tracks in the TPC are projected to the primary vertex, and those passing within 1 cm of the reconstructed primary vertex are used in the analysis. The detector has excellent momentum resolution (the Gaussian width of the track curvature  $k \propto 1/p_T$  is  $\delta k/k = 0.005(p_T/(GeV/c)) + 0.0076$ ), and many sources of secondary tracks (conversions, weak-decays, etc.) are rejected due to the vertex constraint.

For this analysis, we utilize  $\approx 10$  million minimum bias p+p and  $\approx 1.7$  million minimum bias Au+Au events. To augment the central data sample, an additional 1.5 million events triggered on the  $\approx 10\%$  most central collisions are used. For the analysis, we identify events with at least one large transverse momentum track, which we call the trigger particle. The analysis is done for trigger particle thresholds  $3 < p_T^{trig} < 4$ ,  $4 < p_T^{trig} < 6$ , and  $6 < p_T^{trig} < 8$  GeV/c. An azimuthal distribution is constructed for all other charged tracks in these events with  $2 \text{ GeV}/c < p_T < p_T^{trig}$ ,

$$C_2(\Delta\phi) = \frac{1}{N_{trigger}} \frac{1}{\epsilon} \int d\Delta\eta N(\Delta\phi, \Delta\eta), \quad (1)$$

where  $N_{trigger}$  is the observed number of tracks satisfying the trigger requirement, and  $N(\Delta\phi, \Delta\eta)$  is the number of trigger-associated particle pairs as a function of their relative

azimuth ( $\Delta\phi$ ) and pseudo-rapidity ( $\Delta\eta$ ), and  $\epsilon$  is the efficiency for finding the associated track. The analysis is restricted to the range  $|\eta| < 0.7$  ( $|\Delta\eta| < 1.4$ ).

### 3. Fragmentation Contribution to High $p_T$ Particle Production

In order to verify the presence of a hard scattering and fragmentation component at high  $p_T$ , small-angle azimuthal correlations are used [7]. In addition to jets, however, there are other sources of azimuthal correlations. In both p+p and Au+Au collisions, there are azimuthal correlations due to momentum conservation, dijets, and resonance decays. Unique to Au+Au collisions are azimuthal correlations due to elliptic flow. The azimuthal correlations due to momentum conservation, dijets, and elliptic flow should have only a weak pseudo-rapidity dependence within the acceptance window used for this analysis ( $|\eta| < 0.7$ ). To disentangle the sources of azimuthal correlations, the azimuthal distributions can be measured as a function of relative pseudo-rapidity. In the top panel of Figure 1, the azimuthal distributions for central Au+Au collisions are shown for  $|\Delta\eta| < 0.5$  and  $0.5 < |\Delta\eta| < 1.4$ . The small relative pseudo-rapidity azimuthal distribution is absolutely normalized, while the large relative pseudo-rapidity distribution is scaled to match in the region where little correlated jet or dijet contribution is expected ( $0.75 < |\Delta\phi| < 2.24$  radians). There is a clear excess near  $\Delta\phi = 0$  seen at small relative pseudo-rapidity. The bottom panel of Fig. 1 shows the difference in the two distributions. The difference shows the same excess near  $\Delta\phi = 0$ , while showing a flat distribution at larger relative azimuth. From this we conclude that there are correlations localized in  $\Delta\phi, \Delta\eta$ . These correlations are expected from jets and/or resonances.

In order to elucidate the nature (i.e. jets versus resonances) of the small angle correlations in Fig.1, we exploit a known property of jet fragmentation. Dynamical charge correlations exist within jet fragmentation [8]. Leading and next-to-leading charged tracks tend to have opposite charge signs. Figure 2 shows the azimuthal distributions for minimum bias p+p and central Au+Au data for opposite and same sign particle pairs. The p+p data is for  $0 < |\Delta\eta| < 1.4$ . The central Au+Au data is for  $(|\Delta\eta| < 0.5) - N*(0.5 < |\Delta\eta| < 1.4)$ , thereby removing azimuthal correlations due to dijets and elliptic flow. For both the p+p data and central Au+Au data, the correlation strength near  $\Delta\phi = 0$  is larger for opposite sign pairs than for same sign pairs. Integrating the correlation excess, the ratio of opposite sign to same sign peak areas is  $2.7 \pm 0.6$  for p+p data and  $2.4 \pm 0.6$  for central Au+Au data. Phenomenological calculations using Pythia [9] (based on the Lund string fragmentation scheme) predict a ratio of  $2.6 \pm 0.7$ . Large transverse momentum particle production in p+p collisions (and as implemented in the Pythia model) is dominated by hard scattering and fragmentation, so the agreement between central Au+Au, p+p, and Pythia calculations suggests the same underlying particle production mechanism. In addition, the finite same sign azimuthal correlations disfavor the resonance decay hypothesis since only the  $\Delta$  resonance can decay into same sign particle pairs.

### 4. Dijets in Au+Au collisions

Figure 2 also shows clear evidence for back-to-back dihadrons within the STAR acceptance for p+p collisions at  $\sqrt{s} = 200$  GeV/c. The presence of back-to-back dihadrons is an indication of dijets. To compare the dihadron production rates in Au+Au and

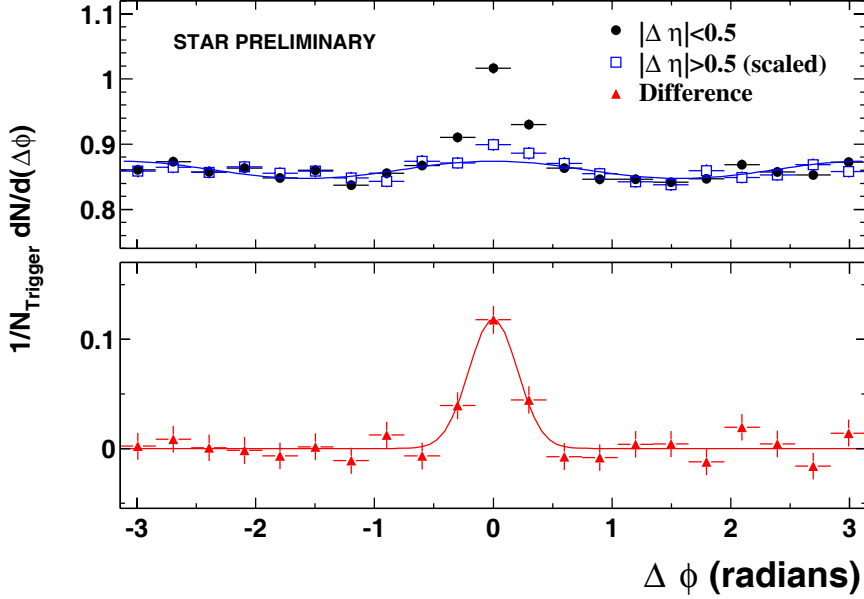


Figure 1. Charged hadron azimuthal distributions for central Au+Au collisions at  $\sqrt{s_{NN}} = 200$  GeV/c. The trigger particle threshold is  $4 < p_T^{\text{trig}} < 6$  GeV/c and the associated particle threshold is  $2 \text{ GeV/c} < p_T < p_T^{\text{trig}}$ . The circles are for  $|\Delta\eta| < 0.5$ , the squares are for  $0.5 < |\Delta\eta| < 1.4$ , and the triangles represent the difference.

p+p collisions, we treat high  $p_T$  triggered Au+Au events as a superposition of a high  $p_T$  triggered p+p collision collision and a combinatorial elliptic flow background,

$$C_2^{\text{AuAu}} = C_2^{\text{pp}} + B(1 + 2v_2(p_T^t)v_2(p_T^a)\cos(2\Delta\phi)), \quad (2)$$

where  $p_T^t(p_T^a)$  is the trigger (associated) particle transverse momentum. The elliptic flow parameters  $v_2$  are measured independently using a reaction plane method [10]. Since  $v_2$  is approximately constant for  $p_T > 2$  GeV/c, a constant value is used. The parameter  $B$  is determined by fitting in the region  $0.75 < |\Delta\phi| < 2.24$ . In Figure 3, we compare the azimuthal distributions in Au+Au at various centralities to the expectation from Eqn. 2. Qualitatively, the Au+Au azimuthal distributions at all centralities are described quite well near  $\Delta\phi = 0$  as the superposition of elliptic flow and p+p azimuthal distributions. In contrast, the back-to-back azimuthal correlations predicted from Eqn. 2 are always larger than the back-to-back correlations seen in the Au+Au data. In the most peripheral Au+Au collisions, the suppression of back-to-back dihadrons is rather small, while for the most central collisions there is little indication of any back-to-back dihadrons beyond those expected from elliptic flow.

As the trigger particle threshold is increased, it might be expected that back-to-back dihadrons reappear. In Figure 4, the azimuthal distribution expected from Eqn. 2 is compared to that measured in central Au+Au events for  $6 < p_T^{\text{trig}} < 8$  GeV/c. Once again, the small angle azimuthal distribution measured in Au+Au is well described by

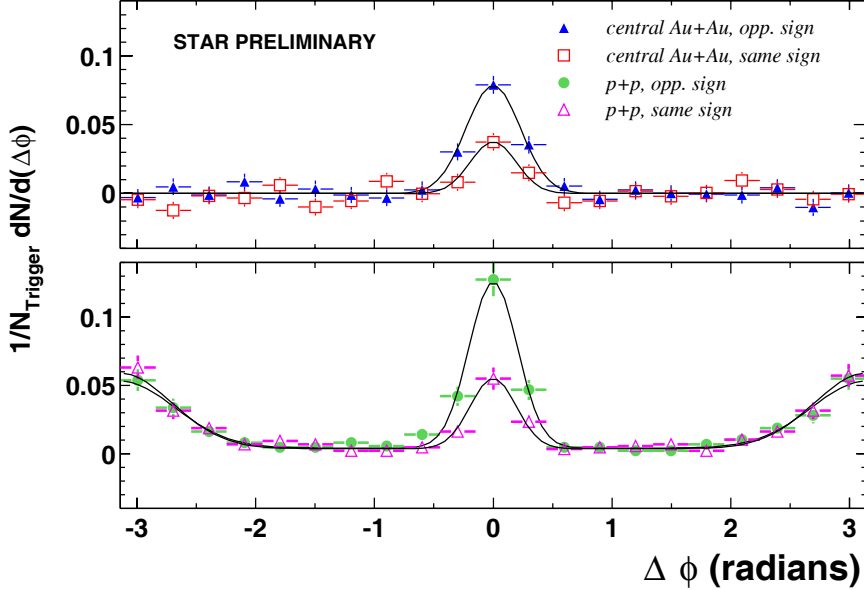


Figure 2. Charged hadron azimuthal distributions for same sign and opposite sign pairs. The top panel shows central Au+Au data ( $|\Delta\eta| < 0.5 - 0.5 < |\Delta\eta| < 1.4(\text{scaled})$ ), and the bottom panel shows p+p data ( $0 < |\Delta\eta| < 1.4$ ). The trigger particle threshold is  $4 < p_T^{\text{trig}} < 6$  GeV/c and the associated particle threshold is  $2 \text{ GeV}/c < p_T < p_T^{\text{trig}}$ .

Equation 2, while there is an absence of back-to-back correlated dihadrons in the central Au+Au data.

To quantify deviations from Eqn. 2, we form a ratio of the Au+Au correlation excess beyond that expected from elliptic flow and the p+p correlation excess,

$$I_{AA}(\Delta\phi_1, \Delta\phi_2) = \frac{\int_{\Delta\phi_1}^{\Delta\phi_2} d(\Delta\phi) [C_2^{\text{AuAu}} - B(1 + 2v_2^t v_2^a \cos(2\Delta\phi))]}{\int_{\Delta\phi_1}^{\Delta\phi_2} d(\Delta\phi) C_2^{\text{pp}}} \quad (3)$$

This ratio is plotted as function of the number of participating nucleons for the small-angle and back-to-back azimuthal regions in Figure 5. The left panel shows the ratios for  $3 < p_T^{\text{trig}} < 4$  GeV/c, the middle panel shows the ratios for  $4 < p_T^{\text{trig}} < 6$  GeV/c, and the right panel shows the ratios for  $6 < p_T^{\text{trig}} < 8$  GeV/c. The horizontal bars show the systematic error on the ratio due the  $+5/-20\%$  systematic uncertainty on the  $v_2$  measurement from the reaction plane method [7]. For all three trigger particle thresholds,  $I_{AA}(0, 0.75)$  is smaller than unity for the most peripheral collisions, and increases with increasing number of participants. The dependence on centrality is strongest for the lowest trigger particle  $p_T$  threshold. In contrast,  $I_{AA}(2.24, \pi)$  decreases with increasing  $N_{\text{part}}$ , and approaches zero for the most central collisions for all three trigger particle thresholds. Note that with increasing trigger particle threshold, the jet and dijet correlation signals increase relative to the elliptic flow contribution, leading to smaller systematic errors on the  $I_{AA}$  determination.

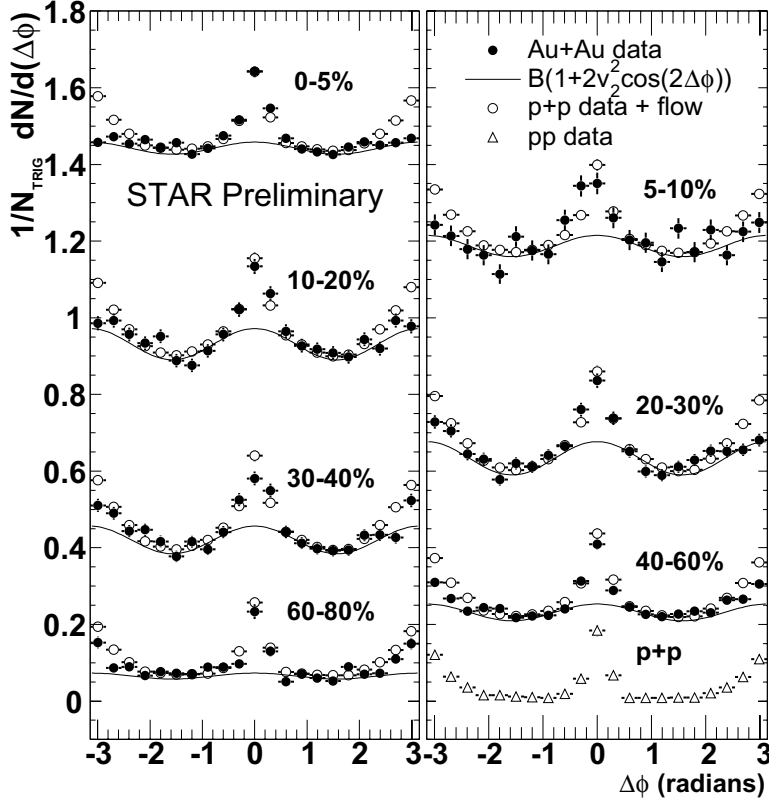


Figure 3. Azimuthal distributions ( $0 < |\Delta\eta| < 1.4$ ) for Au+Au collisions (solid circles) compared to the expected azimuthal distributions from Equation 2 (open circles). The trigger particle threshold is  $4 < p_T^{trig} < 6$  GeV/c and the associated particle threshold is  $2 \text{ GeV}/c < p_T < p_T^{trig}$ . Also shown is the expected elliptic flow contribution for each centrality (solid curve).

It has been shown in fixed target experiments at Fermilab that the shape of the back-to-back dihadron azimuthal distribution is sensitive to the intrinsic parton  $k_T$  [11]. In proton-nucleus and nucleus-nucleus collisions, additional initial state transverse momentum is generated due to multiple nucleon-nucleon interactions. To investigate whether this nuclear  $k_T$  can cause the observed deficit of back-to-back azimuthal correlations in Au+Au collision, the  $k_T$  parameter in Pythia was varied from the nominal value of  $\sigma = 1$  GeV/c to a value of  $\sigma = 4$  GeV/c. This was found to have only a small effect on  $I_{AA}(2.24, \pi)$ , resulting in less than a 20% reduction in the predicted value.

## 5. Discussion and Conclusions

These data on azimuthal correlations and other data on high  $p_T$  particle production at RHIC can be explained with a simple model. The single particle inclusive yields for  $p_T > 2$  GeV/c are suppressed in central Au+Au collisions compared to the binary nucleon-

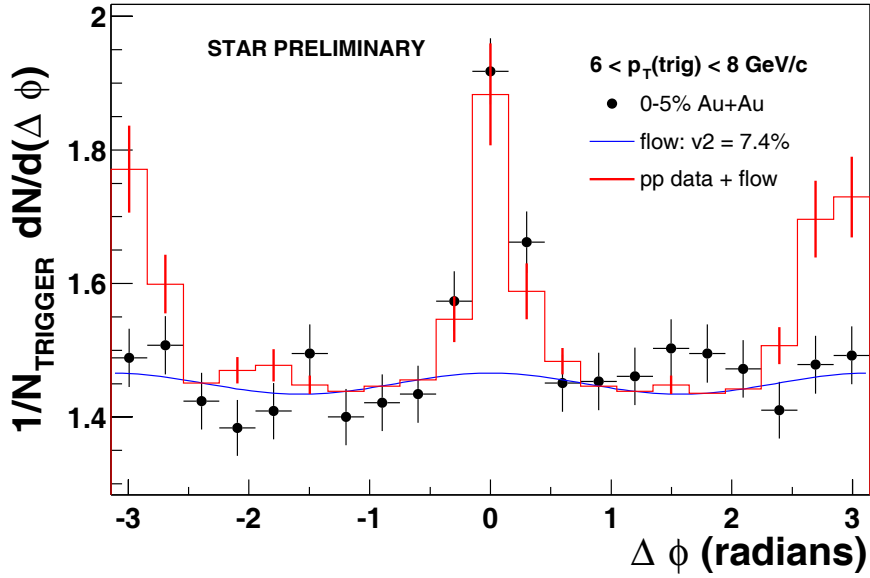


Figure 4. Azimuthal distributions ( $0 < |\Delta\eta| < 1.4$ ) for central Au+Au collisions (solid circles) compared to the expected azimuthal distributions from Equation 2 (histogram). The trigger particle threshold is  $6 < p_T^{trig} < 8$  GeV/c and the associated particle threshold is  $2$  GeV/c  $< p_T < p_T^{trig}$ . Also shown is the expected elliptic flow contribution (solid curve).

nucleon scaling expectation. In addition, the elliptic flow has been shown to saturate above  $p_T \approx 2 - 3$  GeV/c. The measured small angle azimuthal correlations suggest that the properties of the jets we do observe via their leading particles are substantially unmodified by the nuclear medium. These jets most likely come from partons produced near the surface of the collision region. The suppression of single particle inclusive yields and the disappearance of back-to-back dihadron pairs in the most central collisions suggest that partons produced in the center of the collision region, or their hadronic fragments, experience large energy loss or complete absorption. This surface emission scenario was predicted to be a consequence of energy loss [12].

In summary, STAR has measured azimuthal correlations among high  $p_T$  charged hadrons. The small angle correlations provide direct evidence for the dominance of hard scattering and fragmentation processes in high  $p_T$  particle production in Au+Au collisions at RHIC. The observed relative charge sign dependence is consistent with the expectation of parton fragmentation. A simple model treating the azimuthal correlations as a superposition of one hard scattering and elliptic flow is used to compare the rates of back-to-back dihadron production in p+p and all centralities of Au+Au collision. The suppression of back-to-back correlated dihadron pairs varies with centrality and is largest for the most central collisions. These data suggest that high  $p_T$  hadrons come from hard-scattering processes that occur near the edge of the collision region, and that the medium produced in central Au+Au collisions at RHIC is opaque to the propagation of fast partons or their



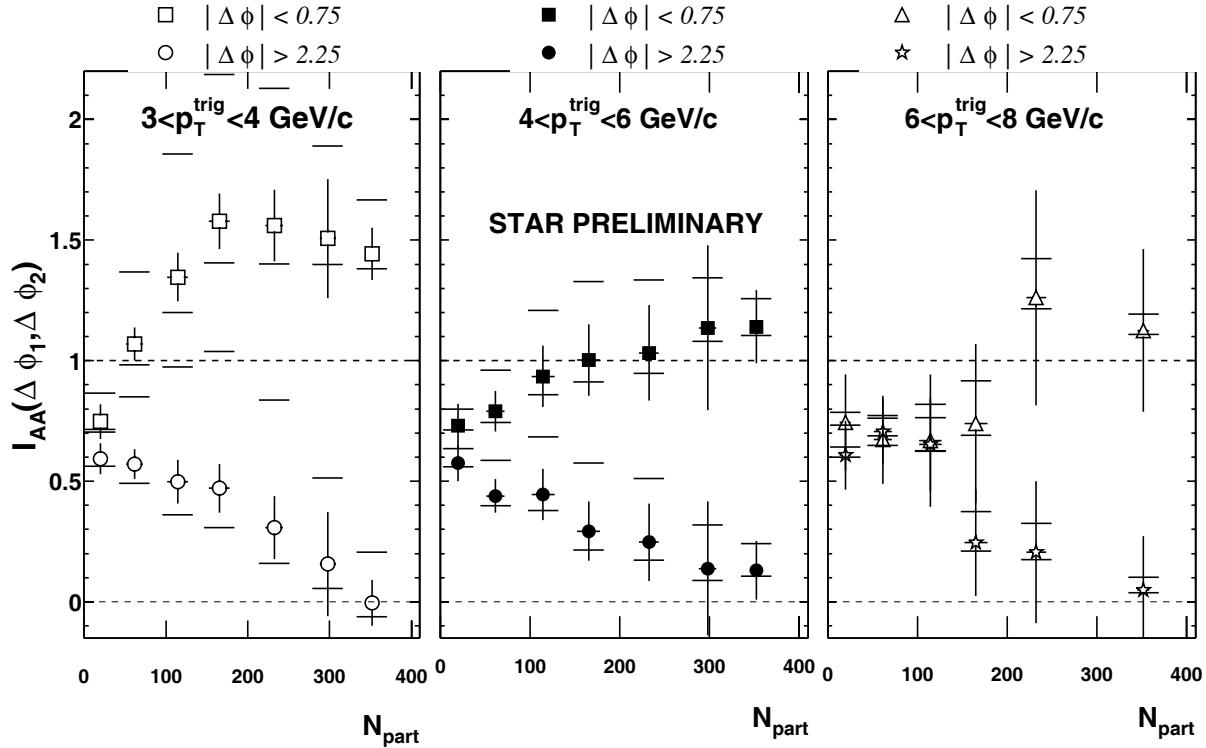


Figure 5.  $I_{AA}$  versus number of participants for small-angle ( $|\Delta\phi| < 0.75$ ) and back-to-back ( $|\Delta\phi| > 2.24$ ) azimuthal regions.

fragmentation products.

## REFERENCES

1. M. Gyulassy and M. Plümer, Phys. Lett. B 243, 432 (1990).
2. X. N. Wang and M. Gyulassy, Phys. Rev. Lett. 68, 1480 (1992).
3. K. Adcox, *et al.*, Phys. Rev. Lett. 88, 022301 (2002).
4. C. Adler, *et al.*, nucl-ex 0206011.
5. T. Sakaguchi, *et al.*, these proceedings.
6. C. Adler, *et al.*, submitted to Nucl. Inst. Meth. (2002).
7. C. Adler, *et al.*, nucl-ex/0206006.
8. P. Abreu, *et al.*, Phys. Lett. B 407, 174 (1997).
9. T. Sjöstrand, P. Edén, C. Friberg, L. Lönnblad, G. Miu, S. Mrenna and E. Norrbin, Comp. Phys. Commun. **135**, 238 (2001).
10. K. Filimonov, these proceedings.
11. L. Apanasevich, *et al.*, Phys. Rev. Lett. 81 (1998) 2642.
12. J.D. Bjorken, Fermilab-Pub-82/59-THY (1982).